The p38 MAPK signaling pathway has been involved in a number of important biological activities, such as proliferation, inflammation, cell death, and aging [18]. The activation of p38 is dependent not only on stimuli but also on cell types. In reproductive cells, it plays a pivotal role in oocyte maturation [19-22] and steroidogenesis [23, 24]. On the other hand, p38, similar to JNK, is known to function as a stress transducer, and is highly activated in aged cells and tissues [25-27]. p38 is activated in klotho knockout mice showing a premature aging phenotype, whereas it is down-regulated in klotho-overexpressing model [28]. In addition, a p38 inhibitor prevented death of fibroblasts from Werner syndrome *in vitro* [29, 30]. Therefore, p38 is involved in ROS-induced cellular damage during aging. Interestingly, p38 is activated in the cytoplasm of aged granulosa cells, whereas it is phosphorylated in the nucleus of younger cells [31]. Since p38 has been shown to translocate between the nucleus and cytoplasm in response to various stimuli [32, 33], the downstream transporters of p38 including MK2, MK5 and TAB-1 [32, 34], must be involved in age-associated change in the subcellular localization of p38.

Some GSTs have been shown to be upregulated through the MAPK pathways as self-defense responses to toxins and growth factors [35, 36]. However, MAPKs that regulate GSTT1 expression and functions have not yet been reported. Furthermore, there is no clear under-standing of the roles of GSTT1 during aging. Therefore, we attempted to determine the direct implications of the MAPK pathways in the expression of GSTT1. We also studied the involvement of GSTT1 in mitochondrial activity.

RESULTS

Regulation of H_2O_2 –induced GSTT1 by p38 MAPK

In our previous studies, we observed age-associated changes in GSTT1 expression in granulosa cells [12], as well as changes in the subcellular localization of p38 [31]. Although H_2O_2 is able to induce these changes *in vitro*, it remains uncertain whether GSTT1 induction by H_2O_2 is controlled through the p38 MAPK signaling pathway. Therefore, we examined the expression of GSTT1 induced by H_2O_2 in the presence or absence of distinct MAPK inhibitors. The immunofluorescence study revealed that GSTT1 was highly upregulated in response to H_2O_2, as has been reported previously (Figure 1). In the cells stimulated with H_2O_2, only SB203580 prevented the upregulation of GSTT1 (Figure 1B: ANOVA, $P < 0.05$). These results strongly suggest that the p38 signaling pathway specifically regulates H_2O_2-induced GSTT1.

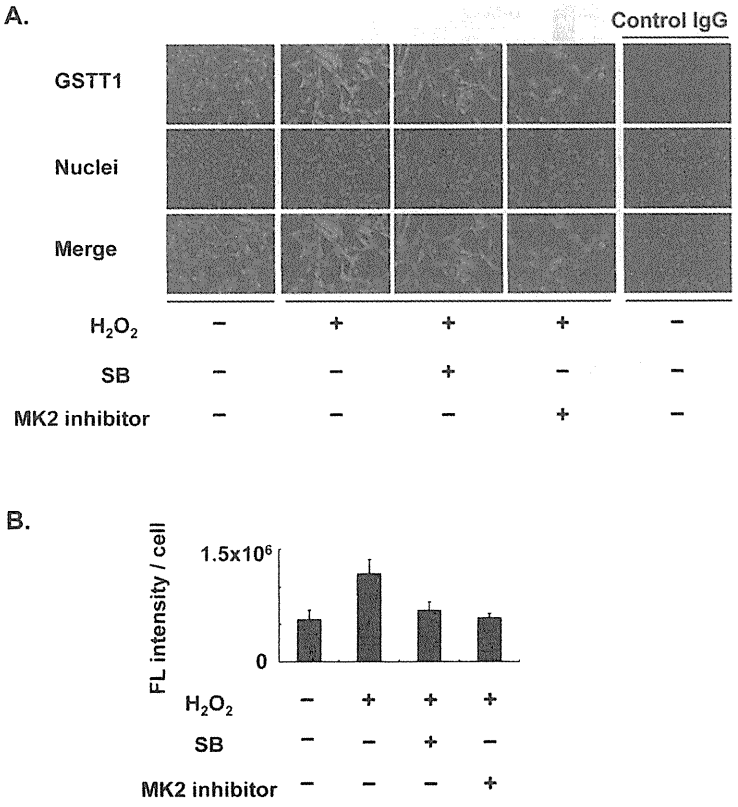

Figure 2. Effects of the MK2 inhibitor on the expression of GSTT1 in KGN cells stimulated with H_2O_2 Cells were treated with H_2O_2 at 200 μM with or without SB203580 at 10 μM or CMPD1 at 330 nM for 24 h and subjected to immunofluorescence analysis (**A**). The primary antibody against GSTT1 was probed with anti-rabbit IgG-Alexa488 (Green). Cells were counterstained with Hoechst 33342 at 10 μM (Blue). Magnification: ×200. A bar graph represent the mean fluorescence intensity per cell ± SEM (**B**, **C**). One-way ANOVA: (**B**) $P < 0.05$; (C) $P < 0.01$.

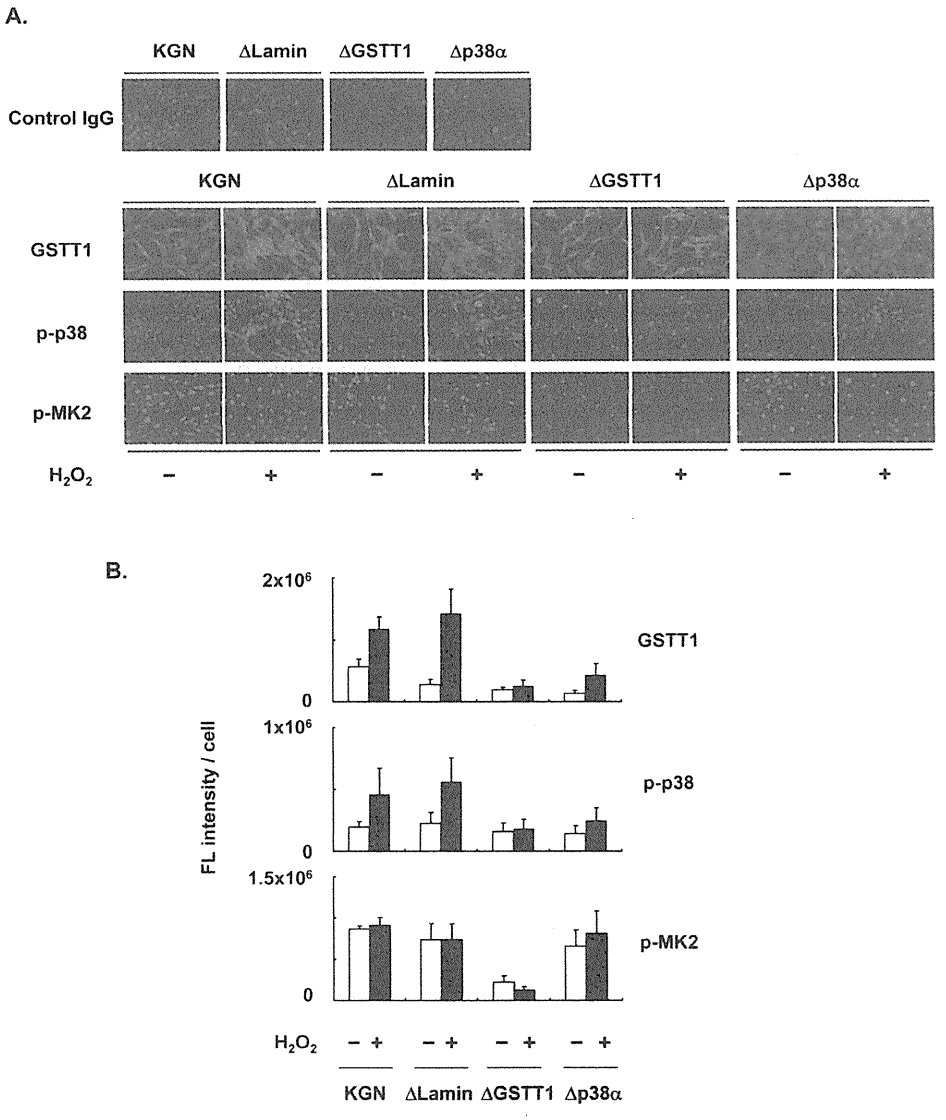

Figure 3. Depletion of GSTT1 inactivates the p38–MK2 signaling pathway. KGN cells (wild–type, ΔLamin ΔGSTT1 or Δp38α cells) were treated with or without H_2O_2 at 200 μM for 24 h before investigation of the expression of GSTT1 and activation of p38 and MK2 by immunofluorescence analysis (**A**). The primary antibodies against GSTT1, phosphorylated p38 and phosphorylated MK2 were probed with anti-rabbit IgG–Alexa488 (Green). Cells were counterstained with Hoechst 33342 at 10 μM (Blue). Magnification: ×200. Bar graphs represent the mean fluorescence intensity per cell ± SEM (**B**). One–way ANOVA: (**B**, GSTT1) $P < 0.001$, (**B**, p-p38) $P < 0.05$, (**B**, p-MK2) $P < 0.001$.

GSTT1 is involved in the p38-MK2 signal cascade under oxidative stress

Since one of the p38 downstream targets, MK2, has been shown to be responsible for both translocation and stress signaling of p38, MK2 may play a role in the regulation of GSTT1 in granulosa cells. KGN cells were therefore pretreated with CMPD1, an MK2 inhibitor, prior to stimulation with H_2O_2 (Figure 2). As expected, CMPD1 blocked GSTT1 induction by H_2O_2 very efficiently, which is very similar to the effects of SB203580 (Figure 2B).

For further analysis of the stress-induced regulation of GSTT1 in granulosa cells, KGN cells stably carrying a knockdown construct of either GSTT1 or p38α were established (ΔGSTT1 and Δp38α cells), and the expression of GSTT1, as well as the phosphorylation of p38 and MK2 was examined for each cell line (Figure 3). H_2O_2 induced GSTT1 expression and phosphorylation of

p38 very efficiently in wild-type and ΔLamin (cells carrying the control vector) cells, whereas both were severely suppressed in ΔGSTT1 and Δp38α cells (Figure 3B). More interestingly, the phosphorylation of MK2 was significantly impaired only in ΔGSTT1 cells and was not even activated by the addition of H_2O_2, suggesting that GSTT1 is highly correlated with MK2 activity.

Supporting the above results, subcellular phosphorylation of p38 in ΔGSTT1 cells differed from that in wild-type and ΔLamin cells (Figure 4). While p38 showed greater phosphorylation in the cytoplasm of wild-type and ΔLamin cells after treatment with H_2O_2, it was unchanged in ΔGSTT1 cells (Figure 4A). In contrast, the nuclear p38 in all cell types was not significantly different before and after treatment with H_2O_2, although it appeared to be increased in ΔLamin and ΔGSTT1 cells compared with wild-type cells (Figure 4B). These results strongly suggest that GSTT1 is involved in the p38-MK2 signaling pathway.

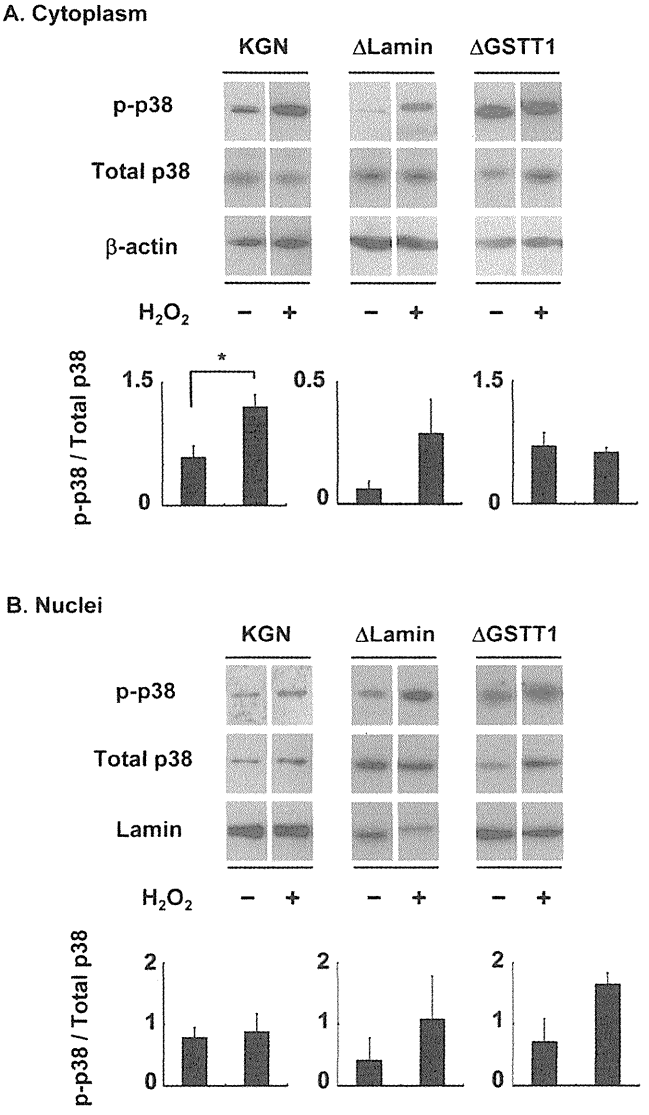

Figure 4. Depletion of GSTT1 prevents the cytoplasmic activation of p38. Cells stimulated with or without H_2O_2 were subjected to fractionation of cytosolic and nuclear proteins. The activity of p38 in each fraction was then analyzed by immunoblotting (**A**: cytoplasm, **B**: nuclei). Fifteen micrograms of total protein were used for each lane. Bar graphs represent the mean band intensity ± SEM. (**A**) Student's *t*–test: $P < 0.05$.

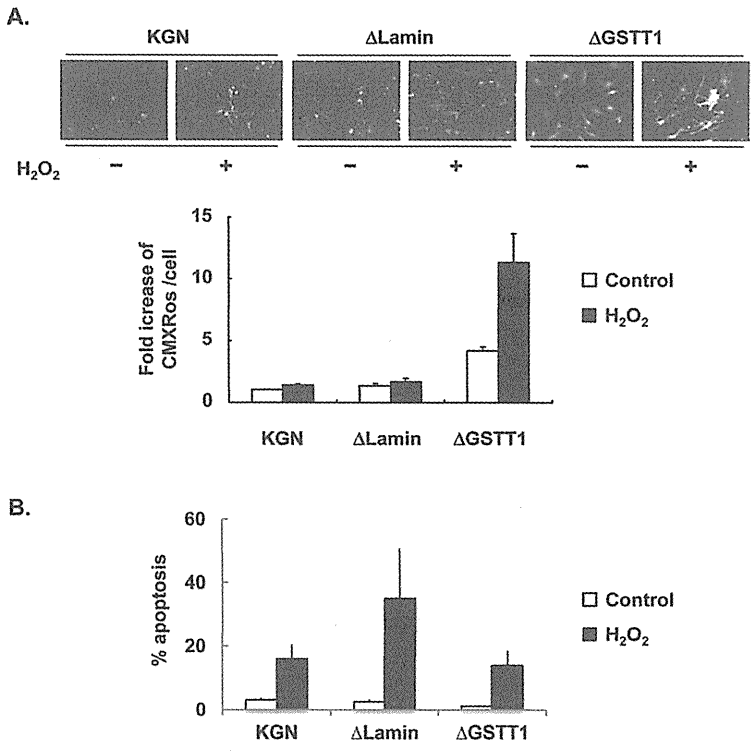

Figure 5. Depletion of GSTT1 enhances mitochondrial activity. (**A**) Wild–type, ΔLamin or ΔGSTT1 cells were stimulated with H_2O_2, and the mitochondrial membrane potential of each cell type was observed by staining with Mitotracker CMXRos at 100 nM. A bar graph represent the fold increase in mean fluorescence intensity ± SEM. One–way ANOVA: $P < 0.001$. (**B**) Frequency of apoptosis before and after treatment with H_2O_2 was measured by TUNEL assay. The number of apoptotic cells was counted and divided by the total number of cells per field. A bar graph represent the frequency of apoptosis ± SEM.

GSTT1 is involved in mitochondrial activity

Because the expression of GSTT1 induced by oxidative stress is mediated through the p38 signaling pathway, GSTT1 may influence the mitochondrial activity. Therefore we examined the $\Delta\Psi m$ of ΔGSTT1 cells using Mitotracker CMXRos. As shown in Figure 5A, suppression of the GSTT1 expression led to a marked increase in the fluorescence intensity of CMXRos under normal conditions. In addition, the mitochondrial hyperpolarity was much more intense in ΔGSTT1 cells compared with wild-type and ΔLamin cells after treatment with H_2O_2.

Since the mitochondrial membrane potential is closely related to cellular viability, the apoptosis of these cells after treatment with 200 μM H_2O_2 was determined by TUNEL assay. As shown in Figure 5B, the viability of ΔGSTT1 cells before and after H_2O_2 treatment was comparable to that of wild-type KGN cells, indicating that the hyperpolarization of $\Delta\Psi m$ observed in ΔGSTT1 cells is not a sign of senescence.

DISCUSSION

Expression of GSTs is directly or indirectly regulated through MAPK pathways. In hepatocytes, GSTM1 and M2 are upregulated by geniposide, an irdoid glycoside, through the ERK signal pathway [36], and an ERK inhibitor was shown to enhance upregulation of GSTA1 by sulforaphane in CaCo-2 cells [37]. In Hep3B cells, GSTA1 has been shown to be induced by alcohol through both ERK and p38 pathways [38]. Similarly, EGF-dependent induction of GSTA4 is mediated by the ERK and p38 pathways [35]. Therefore, the induction of each GST class through distinct MAPK pathways is

likely to be cell type- and stimulus-specific. In this study, GSTT1 was shown to be upregulated in human granulosa cells by oxidative stress only through the p38 signal pathway, suggesting that the interplay between p38 and GSTT1 may be involved in aging of granulosa cells.

MK2 is known to be a direct substrate of p38, and determines the subcellular localization of p38 [39]. Although it remains unclear whether the age-associated subcellular localization of p38 in granulosa cells is caused by the action of MK2, the data shown in Figure 2 indicate not only that oxidative stress-induced GSTT1 is mediated specifically through the p38-MK2 pathway, but also that aged-related functional modifications in granulosa cells may be dependent on the action of MK2. MK2 is regarded as a versatile molecule; it functions in proinflammatory cytokine stabilization [39] and also modulates proteolysis through direct interactions with Hsp27 [40]. These functions are closely associated with the activity and localization of p38. Endogenous p38 is located in both the cytoplasm and nucleus of the resting cells, and cytoplasmic p38 translocates into the nucleus in response to various stimuli [32]. Activated p38 then phosphorylates nuclear MK2 and forms a complex whereby the MK2 nuclear export signal is unmasked, resulting in its rapid export from the nucleus [33, 41]. In contrast, p38 has also been reported to be down-regulated in MK2-deficient tissues [39, 42]. Regarding the amount of total MK2, it was decreased markedly in ΔGSTT1 cells in our preliminary experiments (data not shown). These results may demonstrate that GSTT1 is one of the target molecules for MK2 controlled by the p38 signaling pathway and may be involved in cytokine production. Further study is required.

Fluctuation in $\Delta\Psi m$ is important for mitochondrial activity. $\Delta\Psi m$ is generally accepted to be decreased by the opening of pores in the mitochondrial inner membrane in response to oxidative stress, resulting in apoptotic and necrotic cell death [43]. More precisely, increasing $\Delta\Psi m$ is observed only at the early onset of apoptosis [44], and triggers cytochrome c release into the cytosol, collapse of $\Delta\Psi m$, activation of caspases, and DNA fragmentation [45]. On the contrary, neurons with more hyperpolarization are associated with increased glucose uptake, NADPH availability and increased viability [46]. Also, the following feedback mechanism has been suggested; glucose-induced mitochondrial hyperpolarization leads to a rise in Ca^{2+}, and the increased Ca^{2+} in turn decreases ATP synthesis by mitochondrial depolarization, terminating the influx of Ca^{2+} [47]. Thus, $\Delta\Psi m$ functions as a signal transducer to determine subsequent cellular activities. Although the mechanism underlying the significant increase in $\Delta\Psi m$ in ΔGSTT1 cells remains to be determined, the lowered activity of p38 before and after H_2O_2 treatment in ΔGSTT1 cells may be related to hyperpolarization. In fact, H_2O_2 has been shown to induce activation of p38 and depolarization of $\Delta\Psi m$ in intestinal epithelial cells [48]. These changes were attenuated by pretreatment of cells with SB203580. Similar effects of SB203580 were observed in hepatocytes treated with arachidonic acid, a model for alcohol-induced liver injury [49].

The remaining question relating to our results must be whether or not the increase in $\Delta\Psi m$ observed in the context of lowered GSTT1 is beneficial for granulosa cells. As shown in Figure 5, the hyperpolarization of $\Delta\Psi m$ in ΔGSTT1 cells was not associated with cellular apoptosis. Rather, the increased basal $\Delta\Psi m$ in ΔGSTT1 cells may be due to the enhanced activity of mitochondria, since mitochondria-related steroidogenic genes are upregulated under normal condition (data not shown). The expression of one such gene, steroidogenic acute regulatory protein, is closely related to mitochondrial activity since it is significantly decreased after exposure of cells to oxidative stress [50]. We also observed increased expression of cyclooxygenase 2 in H_2O_2-stimulated ΔGSTT1 cells in our preliminary experiments. Therefore, the observed mitochondrial hyperpolarization may enhance the susceptibility of mitochondria to various external stimuli.

In conclusion, this study demonstrates that oxidative stress-induced upregulation of GSTT1 is mediated through the p38-MK2 signaling pathway. The changes in signal transduction induced by oxidative stress, in turn, influences the mitochondrial activity. Collectively, these results suggest that GSTT1 is associated with reproductive aging through its effects on the p38-MK2 signaling pathway.

MATERIALS AND METHODS

Reagents. Hydrogen peroxide (H_2O_2) was purchased from Wako Pure Chemical Co. Ltd (Tokyo, Japan). Hoechst 33342, protease inhibitor cocktail, phosphatase inhibitors 1 and 2, and a rabbit polyclonal antibody against phosphorylated p38 (Thr180/Tyr182) for the immunofluorescence analysis were purchased from Sigma–Aldrich Inc (Tokyo, Japan). SB203580 (p38 inhibitor) and rabbit polyclonal antibodies against GSTT1 and phosphorylated MK2 (Thr222) were purchased from Santa Cruz Biotechnology Inc (Santa Cruz, CA, USA). SP600125 (JNK inhibitor) was purchased from Enzo Life Sciences, Inc. (Farmingdale, NY, USA). PD98059 (ERK inhibitor) and CMPD1 (4-

(2'- fluorobiphenyl-4-yl) - N -(4- hydroxyphenyl) - butyramide, MK2 inhibitor) were purchased from Merck Ltd. (Tokyo, Japan). A rabbit antibody against phosphorylated p38 (Thr180/Tyr182) for the immunoblot analysis was purchased from Novus Biologicals Inc. (Littleton, CO, USA). A mouse monoclonal antibody against β–actin, a control rabbit IgG, a control mouse IgG, and a donkey anti–mouse IgG conjugated with HRP were purchased from Chemicon International Co. Ltd. (Temecula, CA, USA). A goat anti–rabbit IgG conjugated with HRP was purchased from Thermo Fisher Scientific Inc. (Rockford, IL, USA). A rabbit polyclonal antibody against lamin was purchased from Abcam Inc. (Cambridge, MA, USA). A goat anti–rabbit IgG conjugated with Alexa Flour 488 and MitoTracker CMXRos were purchased from Molecular Probes, Inc. (Eugene, OR, USA).

Cell culture and treatment. The human granulosa–like cell line, KGN, was maintained as described previously [12, 51]. Briefly, cells were cultured in DMEM/F12 containing 1 IU/ml penicillin, 1 μg/ml streptomycin, and 10% heat–inactivated FBS (Biowest Ltd., Nuaille, France, culture medium). Cells were seeded at 5×10^4 cells / ml (200 ml / well) in 8–well culture slides (BD Japan Co. Ltd., Tokyo, Japan) for the subsequent immunofluorescence studies or in culture dishes (Nunc, Roskilde, Denmark) for immunoblot analysis. The medium was replaced by DMEM/F12 containing 0.1% BSA (serum–free medium) before stimulation. The cells were then treated with 200 μM H_2O_2 for 24 h with or without SB203580 (10 μM), SP600125 (10 μM), PD98059 (10 μM) or CMPD1 (330 nM). The final concentrations of inhibitors are determined according to the previous reports in which these inhibitors were used in various cell types [52-54]. After the treatment, they were either fixed or collected and stored as described previously [12, 31].

shRNA design and transfection. To construct shRNA knockdown vectors, the target sequences of the desired genes were synthesized and obtained from Invitrogen Corp. (Carlsbad, CA, USA). GSTT1: Top CACCGCAGGAATGGCTTGCTTAAGACGAATCTT AAGCAAGCCATTCCTGC, Bottom AAAAGCAGG AATGGCTTGCTTAAGATTCGTCTTAAGCAAGCC ATTCCTGC, p38α: Top CACCGCCGAGCTGTTGA CTGGAAGACGAATCTTCCAGTCAACAGCTCGGC, Bottom AAAAGCCGAGCTGTTGACTGAAGATTC GTCTTCCAGTCAACA GCTCGGC, Lamin: Top CACCGCTGGACTTCCAGAAGAACACGAATGTTC TTCTGGAAGTCCAG, Bottom AAAACTGGACTCC AGAAGAACATTCGTGTTCTTCTGGAAGTCCAGC, These oligonucleotides were annealed and cloned into a BLOCK–iT RNAi entry vector (pENTER/U6, Invitrogen Corp.) according to the manufacturer's instruction. After verification by sequencing of the DNA sequence inserted into the vector, the target sequences were transferred into the destination vector (pLenti6/BLOCK–iT-DEST) using the Gateway system (Invitrogen Corp.). Lentiviruses were then produced in 293FT cells using ViraPower Lentiviral Expression Systems, and KGN cells were subjected to lentiviral infection. Cells stably carrying each shRNA construct were maintained in culture medium containing blasticidin at 5 μg/ml. The efficiency of gene knockdown by shRNA was verified by either immunofluorescence or immunoblot analyses.

Immunofluorescence. Immunofluorescence staining was performed as described previously [12]. Briefly, the cells were permeabilized and blocked with Block Ace (Snow Brand Milk Products Co. Ltd., Tokyo, Japan) and treated with the first antibody (10 μg/ml for p-p38 and p-MK2, 20 μg/ml for GSTT1) overnight at 4°C followed by treatment with the secondary antibody (1:200 dilution) for 2 h at room temperature. Hoechst 33342 at 10 μM was also included during treatment with the secondary antibody to enable detection of nuclei. Microphotographs were taken using an epifluorescence microscope equipped with a computational CCD camera (Olympus, Tokyo, Japan). For the image analysis, photographs were taken from five different areas in each sample using the MetaMorph program (Molecular Devices Corp. Tokyo, Japan), and the total fluorescence intensity was measured for each field. The number of cells per field was counted simultaneously by careful observation of Hoechst stained specimens. The normalized fluorescence intensity was then obtained by dividing the total fluorescence intensity by the number of cells in each field. Data were collected from three independent experiments and are shown as the mean fluorescence per cell ± SEM.

Immunoblot analysis. KGN cells were passaged and cultured in a culture medium for 3 days (usually they reach to the sub-confluent status during the culture period) and then maintained for 6 h in a serum-free medium before treatment with H_2O_2 After treatment, the cells were washed twice with Tris-buffered saline (20 mM Tris, pH 7.5, 130 mM NaCl, TBS) containing protease inhibitor and phosphatase inhibitor cocktails and placed on ice as quickly as possible. They were then lysed by direct application of a lysis buffer to the dish.

The nuclear/cytosol fractionation kit (Bio Vision Technology Inc., New Minas, NS, Canada) was used to

separate nuclear and cytoplasmic proteins, according to the manufacturer's protocol. After isolation of the proteins, the concentration of the samples was determined using a micro BCA assay kit (Thermo Fisher Scientific Inc.). Fifteen micrograms of sample per lane were electrophoresed on a 12% reducing SDS-polyacrylamide gel and transferred onto a PVDF membrane (Immobilon-P; Millipore, Tokyo, Japan). After blocking with 10% goat serum and 90% Block Ace at room temperature for 1 h, the membranes were treated with a primary antibody at 1:1000 dilution in TBST and subsequently with a secondary antibody at 1:10,000 dilution. SuperSignal West Femto Maximum Sensitivity Substrate (Thermo Fisher Scientific Inc.) was then used for visualization, and the signal was developed on an X-ray film (GE Healthcare, Piscataway, NJ, USA). The band intensity of phosphorylated p38 was measured using Adobe Photoshop Elements 2.0 software and the background was subtracted. It was then divided by the band intensity of total p38 for normalization. Data were collected from three independent experiments and are shown as the mean changes in band intensity ± SEM.

Measurement of mitochondrial membrane potential ($\Delta\Psi m$). To assess the changes in $\Delta\Psi m$, the cells were treated with or without 200 μM H_2O_2 for 24 h and labeled with the MitoTracker CMXRos probe at 100 nM for 30 min. They were washed twice with TBS and fixed with 4% formaldehyde for 1 h at room temperature. Fluorescence images were taken as described above and the fluorescence intensity of each image was measured with Adobe Photoshop Elements 2.0. It was then divided by the number of cells in each field. The fluorescence intensity per cell was defined as 1.0 for the wild-type KGN cells to obtain fold changes in fluorescence. Data were collected from three independent experiments and are shown as the mean fold increase in fluorescence ± SEM.

Terminal deoxynucleotidyl transferase-mediated dUTP nick end-labeling (TUNEL) assay for apoptosis. Cell apoptosis was detected using TUNEL enzyme and labeling mix according to the manufacturer's instructions (Roche Diagnostics Japan Co. Ltd., Tokyo, Japan). In brief, cells were plated in 8-well culture slides for a couple of days and stimulated with 200 μM H_2O_2 for 24 h as described above. They were then washed with PBS three times and fixed with 2% paraformaldehyde in PBS for 1 h. Next, the cells were permeabilized and labeled with flurescein-dUTP. During the TUNEL labeling Hoechst 33342 at 10 μM was included. The number of flurescein-labeled cells and the total number of cells stained with Hoechst 33342 was counted simultaneously in each field of view under an epi-fluorescence microscope. The incidence of apoptosis was calculated by dividing the number of TUNEL-positive cells by the total number of cells per field. The experiments were repeated three times, and the data are shown as the mean percentage of apoptosis ± SEM.

Statistical analysis. For all immunostaining experiments, statistical analysis was conducted by one-way ANOVA. For the immunoblot analysis, differences in the phosphorylation of p38 in cells treated with or without H_2O_2 were analyzed by Student's t-test or modified Student's t-test (Welch's correction) following an F test. For the analysis of apoptosis, a one-way ANOVA followed by Student's t-test was used. Differences were considered statistically significant if $P < 0.05$. All statistical analyses were performed using Microsoft Excel software.

ACKNOWLEDGEMENTS

We thank Dr. Takashi Horikawa for his technical assistance.

FUNDING

This work was supported partly by a Grant-in Aid for Young Scientists (B) (17791147: MI), partly by a grant from Guangdong Natural Science Foundation (9451063201002116: JQ), partly by a grant of Health Research on Children, Youth and Families from Health and Labour Sciences Research Grants (HS), partly by a Grant-in Aid for Scientific Research (C) (18591818: YT) from the Ministry of Education, Culture, Sports, Science and Technology of Japan, and partly by a grant from Honeybee Research Foundation of Yamada Bee Farm (YT).

CONFLICT OF INTERESTS STATEMENT

The authors have no conflict of interest to declare.

REFERENCES

1. Sheehan D, Meade G, Foley VM, Dowd CA. Structure, function and evolution of glutathione transferases: implications for classification of non-mammalian members of an ancient enzyme superfamily. Biochem J. 2001; 360:1-16.

2. Strange RC, Lear JT, Fryer AA. Glutathione S-transferase polymorphisms: influence on susceptibility to cancer. Chem Biol Interact. 1998; 111-112:351-364.

3. Saadat I, Saadat M. Influence of genetic polymorphisms of glutathione S-transferase T1 (GSTT1) and M1 (GSTM1) on hematological parameters. Mol Biol Rep. 2010; 37:249-253.

4. Ketterer B. A bird's eye view of the glutathione transferase field. Chem Biol Interact. 2001; 138:27-42.

5. Cheng JZ, Singhal SS, Sharma A, Saini M, Yang Y, Awasthi S, et al. Transfection of mGSTA4 in HL-60 cells protects against 4-hydroxynonenal-induced apoptosis by inhibiting JNK-mediated signaling. Arch Biochem Biophys. 2001; 392:197-207.

6. Adler V, Yin Z, Fuchs SY, Benezra M, Rosario L, Tew KD, et al. Regulation of JNK signaling by GSTp. EMBO J. 1999; 18:1321-1334.

7. McElwee JJ, Schuster E, Blanc E, Piper MD, Thomas JH, Patel DS, et al. Evolutionary conservation of regulated longevity assurance mechanisms. Genome Biol. 2007; 8:R132.

8. Ayyadevara S, Engle MR, Singh SP, Dandapat A, Lichti CF, Benes H, et al. Lifespan and stress resistance of Caenorhabditis elegans are increased by expression of glutathione transferases capable of metabolizing the lipid peroxidation product 4-hydroxynonenal. Aging Cell. 2005; 4:257-271.

9. Ayyadevara S, Dandapat A, Singh SP, Benes H, Zimniak L, Shmookler Reis RJ, et al. Lifespan extension in hypomorphic daf-2 mutants of Caenorhabditis elegans is partially mediated by glutathione transferase CeGSTP2-2. Aging Cell. 2005; 4:299-307.

10. Singh SP, Niemczyk M, Saini D, Sadovov V, Zimniak L, Zimniak P. Disruption of the mGsta4 gene increases life span of C57BL mice. J Gerontol A Biol Sci Med Sci. 2010; 65:14-23.

11. van Lieshout EM, Peters WH. Age and gender dependent levels of glutathione and glutathione S-transferases in human lymphocytes. Carcinogenesis. 1998; 19:1873-1875.

12. Ito M, Muraki M, Takahashi Y, Imai M, Tsukui T, Yamakawa N, et al. Glutathione S-transferase theta 1 expressed in granulosa cells as a biomarker for oocyte quality in age-related infertility. Fertil Steril. 2008; 90:1026-1035.

13. Landi S. Mammalian class theta GST and differential susceptibility to carcinogens: a review. Mutat Res. 2000; 463:247-283.

14. Deakin M, Elder J, Hendrickse C, Peckham D, Baldwin D, Pantin C, et al. Glutathione S-transferase GSTT1 genotypes and susceptibility to cancer: studies of interactions with GSTM1 in lung, oral, gastric and colorectal cancers. Carcinogenesis. 1996; 17:881-884.

15. Sherratt PJ, Manson MM, Thomson AM, Hissink EA, Neal GE, van Bladeren PJ, et al. Increased bioactivation of dihaloalkanes in rat liver due to induction of class theta glutathione S-transferase T1-1. Biochem J. 1998; 335 (Pt 3):619-630.

16. He R, Lu J, Miao J. Formaldehyde stress. Sci China Life Sci. 2010; 53:1399-1404.

17. Lin Z, Luo W, Li H, Zhang Y. The effect of endogenous formaldehyde on the rat aorta endothelial cells. Toxicol Lett. 2005; 159:134-143.

18. Zarubin T, Han J. Activation and signaling of the p38 MAP kinase pathway. Cell Res. 2005; 15:11-18.

19. Yamashita Y, Hishinuma M, Shimada M. Activation of PKA, p38 MAPK and ERK1/2 by gonadotropins in cumulus cells is critical for induction of EGF-like factor and TACE/ADAM17 gene expression during in vitro maturation of porcine COCs. J Ovarian Res. 2009; 2:20.

20. Villa-Diaz LG, Miyano T. Activation of p38 MAPK during porcine oocyte maturation. Biol Reprod. 2004; 71:691-696.

21. Takenaka K, Moriguchi T, Nishida E. Activation of the protein kinase p38 in the spindle assembly checkpoint and mitotic arrest. Science. 1998; 280:599-602.

22. Salhab M, Tosca L, Cabau C, Papillier P, Perreau C, Dupont J, et al. Kinetics of gene expression and signaling in bovine cumulus cells throughout IVM in different mediums in relation to oocyte developmental competence, cumulus apoptosis and progesterone secretion. Theriogenology. 2011; 75:90-104.

23. Manna PR, Stocco DM. The role of specific mitogen-activated protein kinase signaling cascades in the regulation of steroidogenesis. J Signal Transduct. 2011; 2011:821615.

24. Inagaki K, Otsuka F, Miyoshi T, Yamashita M, Takahashi M, Goto J, et al. p38-Mitogen-activated protein kinase stimulated steroidogenesis in granulosa cell-oocyte cocultures: role of bone morphogenetic proteins 2 and 4. Endocrinology. 2009; 150:1921-1930.

25. Yoon SO, Yun CH, Chung AS. Dose effect of oxidative stress on signal transduction in aging. Mech Ageing Dev. 2002; 123:1597-1604.

26. Savage MJ, Lin YG, Ciallella JR, Flood DG, Scott RW. Activation of c-Jun N-terminal kinase and p38 in an Alzheimer's disease model is associated with amyloid deposition. J Neurosci. 2002; 22:3376-3385.

27. Maruyama J, Naguro I, Takeda K, Ichijo H. Stress-activated MAP kinase cascades in cellular senescence. Curr Med Chem. 2009; 16:1229-1235.

28. Hsieh CC, Kuro-o M, Rosenblatt KP, Brobey R, Papaconstantinou J. The ASK1-Signalosome regulates p38 MAPK activity in response to levels of endogenous oxidative stress in the Klotho mouse models of aging. Aging. 2010; 2:597-611.

29. Davis T, Haughton MF, Jones CJ, Kipling D. Prevention of accelerated cell aging in the Werner syndrome. Ann N Y Acad Sci. 2006; 1067:243-247.

30. Davis T, Baird DM, Haughton MF, Jones CJ, Kipling D. Prevention of accelerated cell aging in Werner syndrome using a p38 mitogen-activated protein kinase inhibitor. J Gerontol A Biol Sci Med Sci. 2005; 60:1386-1393.

31. Ito M, Miyado K, Nakagawa K, Muraki M, Imai M, Yamakawa N, et al. Age-associated changes in the subcellular localization of phosphorylated p38 MAPK in human granulosa cells. Mol Hum Reprod. 2010; 16:928-937.

32. Gong X, Ming X, Deng P, Jiang Y. Mechanisms regulating the nuclear translocation of p38 MAP kinase. J Cell Biochem. 2010; 110:1420-1429.

33. Engel K, Kotlyarov A, Gaestel M. Leptomycin B-sensitive nuclear export of MAPKAP kinase 2 is regulated by phosphorylation. EMBO J. 1998; 17:3363-3371.

34. Lu G, Kang YJ, Han J, Herschman HR, Stefani E, Wang Y. TAB-1 modulates intracellular localization of p38 MAP kinase and downstream signaling. J Biol Chem. 2006; 281:6087-6095.

35. Desmots F, Rissel M, Gilot D, Lagadic-Gossmann D, Morel F, Guguen-Guillouzo C, et al. Pro-inflammatory cytokines tumor necrosis factor alpha and interleukin-6 and survival factor epidermal growth factor positively regulate the murine GSTA4 enzyme in hepatocytes. J Biol Chem. 2002; 277:17892-17900.

36. Kuo WH, Chou FP, Young SC, Chang YC, Wang CJ. Geniposide activates GSH S-transferase by the induction of GST M1 and GST M2 subunits involving the transcription and phosphorylation of MEK-1 signaling in rat hepatocytes. Toxicol Appl Pharmacol. 2005; 208:155-162.

37. Svehlikova V, Wang S, Jakubikova J, Williamson G, Mithen R, Bao Y. Interactions between sulforaphane and apigenin in the induction of UGT1A1 and GSTA1 in CaCo-2 cells. Carcinogenesis. 2004; 25:1629-1637.

38. Zhang D, Lu H, Li J, Shi X, Huang C. Essential roles of ERKs and p38K in up-regulation of GST A1 expression by Maotai content in

human hepatoma cell line Hep3B. Mol Cell Biochem. 2006; 293:161-171.

39. Kotlyarov A, Yannoni Y, Fritz S, Laass K, Telliez JB, Pitman D, et al. Distinct cellular functions of MK2. Mol Cell Biol. 2002; 22:4827-4835.

40. Knapinska AM, Gratacos FM, Krause CD, Hernandez K, Jensen AG, Bradley JJ, et al. Chaperone Hsp27 modulates AUF1 proteolysis and AU-rich element-mediated mRNA degradation. Mol Cell Biol. 2011; 31:1419-1431.

41. Ben-Levy R, Hooper S, Wilson R, Paterson HF, Marshall CJ. Nuclear export of the stress-activated protein kinase p38 mediated by its substrate MAPKAP kinase-2. Curr Biol. 1998; 8:1049-1057.

42. Gorog DA, Jabr RI, Tanno M, Sarafraz N, Clark JE, Fisher SG, et al. MAPKAPK-2 modulates p38-MAPK localization and small heat shock protein phosphorylation but does not mediate the injury associated with p38-MAPK activation during myocardial ischemia. Cell Stress Chaperones. 2009; 14:477-489.

43. Lemasters JJ, Qian T, Bradham CA, Brenner DA, Cascio WE, Trost LC, et al. Mitochondrial dysfunction in the pathogenesis of necrotic and apoptotic cell death. J Bioenerg Biomembr. 1999; 31:305-319.

44. Chandra D, Liu JW, Tang DG. Early mitochondrial activation and cytochrome c up-regulation during apoptosis. J Biol Chem. 2002; 277:50842-50854.

45. Sanchez-Alcazar JA, Ault JG, Khodjakov A, Schneider E. Increased mitochondrial cytochrome c levels and mitochondrial hyperpolarization precede camptothecin-induced apoptosis in Jurkat cells. Cell Death Differ. 2000; 7:1090-1100.

46. Ward MW, Huber HJ, Weisova P, Dussmann H, Nicholls DG, Prehn JH. Mitochondrial and plasma membrane potential of cultured cerebellar neurons during glutamate-induced necrosis, apoptosis, and tolerance. J Neurosci. 2007; 27:8238-8249.

47. Krippeit-Drews P, Dufer M, Drews G. Parallel oscillations of intracellular calcium activity and mitochondrial membrane potential in mouse pancreatic B-cells. Biochem Biophys Res Commun. 2000; 267:179-183.

48. Zhou Y, Wang Q, Mark Evers B, Chung DH. Oxidative stress-induced intestinal epithelial cell apoptosis is mediated by p38 MAPK. Biochem Biophys Res Commun. 2006; 350:860-865.

49. Wu D, Cederbaum AI. Role of p38 MAPK in CYP2E1-dependent arachidonic acid toxicity. J Biol Chem. 2003; 278:1115-1124.

50. Diemer T, Allen JA, Hales KH, Hales DB. Reactive oxygen disrupts mitochondria in MA-10 tumor Leydig cells and inhibits steroidogenic acute regulatory (StAR) protein and steroidogenesis. Endocrinology. 2003; 144:2882-2891.

51. Imai M, Muraki M, Takamatsu K, Saito H, Seiki M, Takahashi Y. Spontaneous transformation of human granulosa cell tumours into an aggressive phenotype: a metastasis model cell line. BMC Cancer. 2008; 8:319.

52. Steffel J, Akhmedov A, Greutert H, Luscher TF, Tanner FC. Histamine induces tissue factor expression: implications for acute coronary syndromes. Circulation. 2005; 112:341-349.

53. Chou SF, Chang SW, Chuang JL. Mitomycin C upregulates IL-8 and MCP-1 chemokine expression via mitogen-activated protein kinases in corneal fibroblasts. Invest Ophthalmol Vis Sci. 2007; 48:2009-2016.

54. Davidson W, Frego L, Peet GW, Kroe RR, Labadia ME, Lukas SM, et al. Discovery and characterization of a substrate selective p38alpha inhibitor. Biochemistry. 2004; 43:11658-11671.

Veterinary Microbiology 154 (2012) 222–229

Contents lists available at ScienceDirect

Veterinary Microbiology

journal homepage: www.elsevier.com/locate/vetmic

Epizootic canine distemper virus infection among wild mammals

Yuki Kameo [a,1], Yumiko Nagao [a,1], Yohei Nishio [a], Hiroshi Shimoda [a], Hitoshi Nakano [a], Kazuo Suzuki [b], Yumi Une [c], Hiroshi Sato [d], Masayuki Shimojima [a], Ken Maeda [a,*]

[a] Laboratory of Veterinary Microbiology, Faculty of Agriculture, Yamaguchi University, 1677-1 Yoshida, Yamaguchi 753-8515, Japan
[b] Hikiiwa Park Center, 1629 Inari-cho, Tanabe 646-0051, Japan
[c] Laboratory of Veterinary Pathology, Azabu University, 1-17-71 Fuchinobe, Kanagawa 229-8591, Japan
[d] Laboratory of Veterinary Parasitology, Faculty of Agriculture, Yamaguchi University, 1677-1 Yoshida, Yamaguchi 753-8515, Japan

ARTICLE INFO

Article history:
Received 9 February 2011
Received in revised form 4 July 2011
Accepted 11 July 2011

Keywords:
Canine distemper
Deer
Raccoon
Raccoon dog
Wild boar

ABSTRACT

In the spring of 2007, seven raccoon dogs and a weasel were captured near the city of Tanabe in Wakayama prefecture, Japan. The causative agent of the animals' death 1–2 days after capture was identified as canine distemper virus (CDV) by virus isolation, immunostaining with an anti-CDV polyclonal antibody, and a commercially available CDV antigen-detection kit. Sequence analysis of hemagglutinin genes indicated the isolated viruses belong to genotype Asia-1 and possess the substitution from tyrosine (Y) to histidine (H) at position 549 that is associated with the spread of CDV to non-canine hosts. A serosurvey for CDV was then conducted among wild animals in the region. The animals assayed consisted of 104 raccoons, 41 wild boars, 19 raccoon dogs, five Sika deer, two badgers, one weasel, one marten, one Siberian weasel and one fox. Virus-neutralization (VN) tests showed that, except for fox and weasel, all of the species assayed had VN antibodies to CDV. Interestingly, 11 of the 41 wild boars (27%) and two of the five Sika deer assayed possessed VN antibodies to CDV. These findings indicate that CDV infection was widespread among wild mammals during this epizootic.

1. Introduction

Canine distemper virus (CDV) is a non-segmented, negative-stranded, enveloped RNA virus of the order *Mononegavirale*, family *Paramyxoviridae* and genus *Morbillivirus*. CDV infects dogs and a variety of carnivore species, causing a fatal disease that manifests as pyrexia, anorexia, nasal discharge, conjunctivitis, diarrhea, leukopenia, and encephalitis (Appel, 1969; Appel and Summers, 1995). Vaccination with attenuated live virus is typically used to protect domestic dogs and cases of dog deaths by CDV are currently rare in Japan. However, CDV strains that are genetically distinct from the one used to produce the live vaccine (Onderstepoort strain), have recently been isolated in different regions of the world, and at least two of these strains, genotypes Asia-1 and Asia-2, have spread throughout Asia and Japan (Mochizuki et al., 1999).

Epizootics of CDV in wild animals are considered to be a serious global problem. For example, the famous discovery of a "mass grave" of lions (*Panthera leo*; Felidae) in the Serengeti National Park of Tanzania in 1994 was later attributed to CDV infection (Roelke-Parker et al., 1996). In California, the island fox (*Urocyon littoralis*) has become endangered due to CDV epizootics (United States Fish and Wildlife Service, 2004; Timm et al., 2009). In Japan, CDV infections have been reported in wild animals from a variety of regions (Machida et al., 1992, 1993; Ohashi et al., 2001; Hirama et al., 2004; Watabe and Yoshizawa, 2006; Yoshizawa and Watabe, 2007; Takayama et al., 2009). In 2008, CDV cases were reported in rhesus monkeys and crab-eating monkeys in China and Japan, respectively

* Corresponding author. Tel.: +81 83 933 5887; fax: +81 83 933 5887.
E-mail address: kmaeda@yamaguchi-u.ac.jp (K. Maeda).
[1] Yuki Kameo and Yumiko Nagao contributed equally to this study.

0378-1135/$ – see front matter © 2011 Elsevier B.V. All rights reserved.
doi:10.1016/j.vetmic.2011.07.006

(Morikawa et al., 2008; Sun et al., 2010). This study reports the findings of a CDV serological survey that was conducted among wild animals after a CDV epizootic in the vicinity of Tanabe in Wakayama prefecture, Japan, in 2007.

2. Materials and methods

2.1. CDV epizootic

Several raccoon dog deaths were reported since the end of March, 2007 around Tanabe in Wakayama Prefecture, Japan. The raccoon dogs presented with prostration and an inability move, and died within 1–2 days after being sheltered. Raccoon dog No. 729 died on April 16, 2007, was sent to Yamaguchi University for diagnosis of the causative agent. A total of seven raccoon dogs and one weasel (No.734) were subsequently diagnosed as being infected with CDV. Although no further cases were reported after May 16, 2007, one raccoon dog (No.812) from the same area died due to CDV infection on January 2008. The characteristics of these infections are summarized in Table 1.

2.2. Cells

Vero cells (Japanese Collection of Research Bioresources (JCRB) Number: JCRB9013) were cultured in Eagle's minimum essential medium (EMEM; Gibco, USA) with 5% heat-inactivated fetal calf serum (FCS; Gibco), 1 mM sodium pyruvate, 100 U/ml penicillin and 100 μg/ml streptomycin at 37 °C in 5% CO_2. Canine A72 cells (American Type Culture Collection (ATCC) Number: CRL-1542), feline CRFK cells (ATCC Number: CCL-94), and A72/cSLAM and CRFK/cSLAM cells expressing canine SLAM (Nakano et al., 2009a,b) were grown in Dulbecco's modified Eagle's medium (DMEM; Gibco) supplemented with 10% FCS and antibiotics at 37 °C in 5% CO_2.

2.3. Viruses

CDV KDK-1 (genotype Asia-1) (Mochizuki et al., 1999) strain was propagated in A72/cSLAM cells, and the Onderstepoort strain (vaccine) was propagated in Vero cells. W729B and W812B strains were isolated from the brains of raccoon dogs No.729 and No.812 in Wakayama Prefecture in 2007 and 2008, respectively, and then isolated and propagated in A72/cSLAM cells.

2.4. Virus isolation

DMEM containing high concentrations of antibiotics was added to swabs and tissues and then vortexed or homogenized. The samples were centrifuged and the supernatants were filtrated through a 0.45 μm filter. The filtrates or sera were then used to inoculate A72/cSLAM cells expressing canine SLAM. The inoculated cells were cultured until cytopathic effect was observed.

2.5. Serum samples

A total of 129 sera were collected from wild animals captured around Tanabe in Wakayama Prefecture from 2007 to 2008. Wild animals included 104 raccoons (*Procyon lotor*), 19 raccoon dogs (*Nyctereutes procyonoides*), two badgers (*Meles meles*), one weasel (*Mustela itatsi*), one Japanese marten (*Martes melampus*), one Siberian weasel (*Mustela sibirica*), one red fox (*Vulpes vulpes*), 41 wild boars (*Sus scrofa*) and five Sika deer (*Cervus nippon*). Furthermore, 28 and 20 sera were collected from wild boars and Sika deer, respectively, captured around Tanabe in Wakayama Prefecture from 2009 to 2010. All sera were heat-inactivated at 56 °C for 30 min and stored at −20 °C until use.

2.6. Virus neutralizing (VN) test

VN test for KDK-1 was performed by a 75% plaque-reduction neutralizing test ($PRNT_{75}$) using our established cell line, CRFK/cSLAM (Nakano et al., 2009a,b). For the first screening of CDV-positive sera, 10 μl of sera was added to 90 μl of virus solution containing approximately 100 plaque forming units (PFU) of KDK-1 diluted with DMEM supplemented with 2% FCS and incubated at 37 °C for 1 h (1:10 dilution). Then, 50 μl of the mixture was added to each well of a 24-well plate (Sumilon, Japan) subconfluented with CRFK/cSLAM. The plate was incubated at 37 °C for 1 h, washed twice with DMEM without FCS and overlaid with DMEM containing 0.8% agarose and 7% FCS. Plates were then incubated at 37 °C in 5% CO_2 for 3–4 days.

Table 1
Characteristics of virus isolates.

No.	Species	Date (yr/m/d)	Sex	Body weight (kg)	Virus isolate[a]	CDV antigen[b]
729	Raccoon dog	2007/4/16	M[c]	2.35	B, U	N.D.[d]
731	Raccoon dog	2007/4/20	F	2.80	F	+
734	Weasel	2007/4/25	M	0.50	B	+
739	Raccoon dog	2007/5/11	F	3.05	–	+
741	Raccoon dog	2007/5/15	F	3.00	F	+
742	Raccoon dog	2007/5/15	F	3.30	–	+
743	Raccoon dog	2007/5/15	F	2.25	U, F	+
744	Raccoon dog	2007/5/16	M	2.20	U, F	+
812	Raccoon dog	2008/1/31	F	2.35	B, U, F, S	+

[a] CDV were isolated from brain (B), fecal sample (F), urine (U) and/or serum (S).
[b] CDV antigen was detected by Checkman CDV and/or immunohistopathology using a CDV-specific polyclonal antibody.
[c] M, male and F, female.
[d] N.D.: not done.

Cells were fixed with 5% buffered formaldehyde for 1 h before agarose layers were removed. Plaques were counted after staining with crystal violet. Compared to the mean number of plaques in control wells, sera that reduced the number of plaques by more than 75% were considered to be positive.

In order to determine the VN titers of CDV-positive sera, sera were diluted to 1:5 and then serially diluted twofold with DMEM containing 2% FCS. Diluted sera were then mixed with equal volumes of virus solution containing 100 PFU of the KDK-1 or Onderstepoort strains, followed by incubation at 37 °C for 60 min. Mixtures were added to CRFK/cSLAM and $PRNT_{75}$ was performed. Compared to control wells without serum, the titer of VN antibody was expressed as the highest dilution of serum that reduced more than 75% of the plaques.

2.7. RT-PCR and hemagglutinin (H) gene sequencing

Total RNA was extracted from virus-infected cells using a QIAGEN RNA Mini kit (QIAGEN, Germany). Reverse-transcription (RT) was carried out with a random 9-mer primer using TaKaRa RNA LA PCR™ kit (AMV) Ver.1.1 (Takara, Japan). The H gene was amplified using primers 204b (5′-GAA TTC GAT TTC CGC GAT CTC C-3′) and 232b (5′-TAG GCA ACA CCA ATA ATT TRG ACT C-3′) (Martella et al., 2007). Amplification was performed using a temperature cycling protocol consisting of 40 cycles of denaturation for 30 s at 94 °C, primer annealing for 30 s at 50 °C, and extension for 1.5 min at 72 °C, followed by a final extension step of 15 min at 72 °C. The amplified products were purified using a QIAquick PCR Purification kit (QIAGEN) and nucleotide sequences were determined using an ABI PRISM 310 Genetic Analyzer autosequencer (Applied Biosystems, CA, USA).

To determine the nucleotide sequence of the complete H genes in W729B and W812B, H genes were amplified using primers CDV-HR (5′-AGA TGG ACC TCA GGG TAT AG-3′) and CDV-HF (5′-AAC TTA GGG CTC AGG TAG TC-3′) (Demeter et al., 2007). The amplified products were purified using a QIAquick PCR Purification kit (QIAGEN) and nucleotide sequences were determined by ABI PRISM 310 Genetic Analyzer autosequencer (Applied Biosystems). For sequence analysis, the H gene primers, HF, HR, 1F (5′-AGG TAT GTA CTA TAG CAG TG-3′), 2F (5′-TAG TAA CCT GGA TGG TGC CT-3′), 3F (5′-CCA GGG AAT CAA GTG GAA AT-3′), 4F (5′-CTC CAT ATC CTC TTT CAG CA-3′), 5F (5′-TCG AAC TCC AGT GAT GGC AA-3′), 204b, 1R (5′-AGG CAC CAT CCA GGT TAC TA-3′), 2R (5′-CAC TGC TAT AGT ACA TAC CT-3′), 3R (5′-TTT TGA CCC CAA CTG CAT CG-3′) and 232b were used.

2.8. Sequence analysis of fusion (F) protein signal peptide

To amplify the signal peptide region of the F gene, RT reaction was carried out as described above. PCR was performed using primers CDV-5668R (5′-GCA GTG ATT TGT GCA GCT GT-3′) and CDV-4713F (5′-TCG CCT CTA GGA ATC TCA CT-3′) and a temperature cycling profile consisting of an initial denaturation step of 2 min at 94 °C followed by 30 cycles of denaturation for 30 s at 94 °C, annealing for 30 s at 60 °C, extension for 1 min at 72 °C, and a final extension step of 15 min at 72 °C. The amplified products were purified as described for the H gene. For the sequence analysis, primers CDV-4713F, CDV-5668R, 5275F (5′-AAC TCA GGC TCT CAG TGC A-3′) and 5283R (5′-TGC ACT GAG AGC CTG AGT T-3′) were used.

2.9. Histopathology and immunostaining

For histopathological examination, specimens of various tissues were fixed in 10% neutral buffered formalin and embedded in paraffin wax. Sections (3 μm) were stained with hematoxylin and eosin (HE). Immunostaining was performed using polyclonal antibody against CDV (Ikeda strain). Secondary reactions were performed with a peroxidase-conjugated Histofine-Simple stain kit (Simplestain MAX-PO; Nichirei, Tokyo), with 3,3′-diaminobenzidine and H_2O_2 used to visualize the reaction products. Slides were counterstained with Mayer's hematoxylin. For negative controls, the primary antibody was omitted.

2.10. Statistical analysis

Chi-square and Fisher's exact probability tests were used for the statistical analysis. The level of significance was $p < 0.05$.

3. Results

3.1. CDV epizootic in wild animals

Seven raccoon dogs (Nos.729, 731, 739, 741, 742, 743, 744) and one weasel (No.734) were captured around Tanabe in Wakayama Prefecture, Japan from April to May in 2007 (Table 1). The animals, which were prostrate and could not move (Supplementary Fig. S1), died within 1–2 days after capture. There were no clinical signs of infection except for diarrhea (Supplementary Fig. S1).

To the best of our knowledge, no instances of epizootic CDV infection in wild animals have previously been reported near Tanabe, and with the exception of one raccoon dog (No.812) that was captured on January 31, 2008, no CDV cases have been reported from the area since May 16, 2007. Using fecal or oral swabs, all of the animals examined using Checkman CDV kits were positive for the CDV antigen (Table 1).

3.2. Virus isolation from raccoon dogs and a weasel

The characteristics of the virus isolates used in this study are listed in Table 1. CDV was isolated from seven animals and two raccoon dogs (No.739 and No.742) were negative for virus isolation. Specifically, five CDV isolates originated from feces, four viruses from urine, three from brains, and only one from serum. Two isolates (W729B and W812B), which were obtained from the brains of raccoon dogs No.729 and No.812, respectively, were used as representative isolates.

To confirm whether the isolated viruses were CDV, RT-PCR and sequence analysis were performed using primers 232b and 204b (Martella et al., 2007). Sequence analysis

Table 2
Summary of histopathology and immunostaining with a polyclonal antibody to CDV.

No.	Bronchus	Alveolus	Tongue	Esophagus	Stomach	Small intestine	Large intestine	Renal pelvis	Bladder	Lymph node	Cerebrum	Cerebellum
734	++	–	–	+	++	–	–	–	–	++	++	–
739	++	+	–	–	–	–	–	–	–	–	–	–
741	–	+	–	–	–	+	–	–	–	–	–	–
742	–	–	–	–	–	++	++	–	–	++	–	–
743	++	+	–	–	+	++	++	++	++	++	–	–
744	–	–	–	–	–	+	+	–	++	–	–	–
812	++	+	+	+	++	++	++	++	++	++	++	++

+, CDV-antigen positive; ++, inclusion body with CDV antigen; –, CDV-antigen negative.

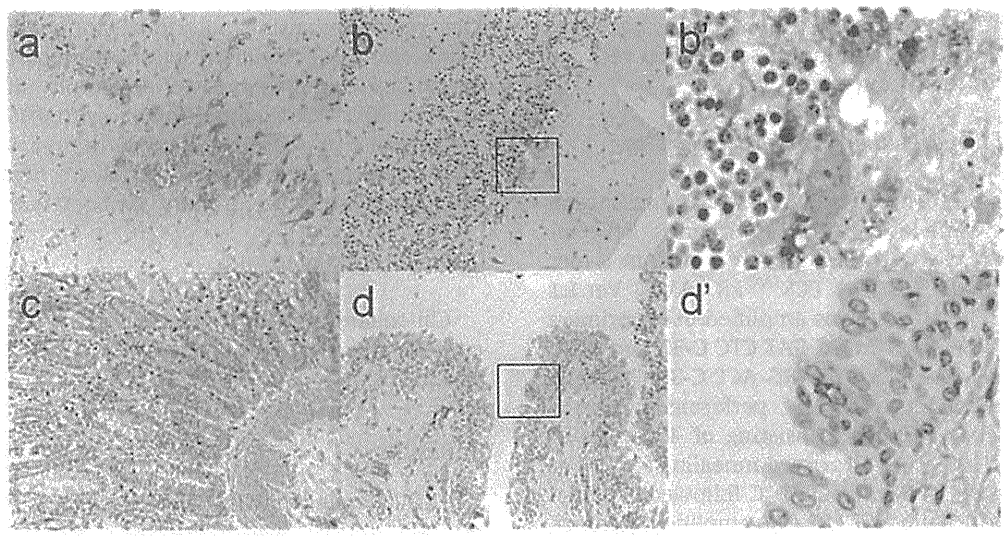

Fig. 1. Immunostaining of CDV antigen in raccoon dog No. 812. (a) cerebrum, (b) cerebellum, (c) large intestine, (d) urinary bladder, (b') magnification of tissue section enclosed by the inset in (b), (d') magnification of tissue section enclosed by the inset in (d).

showed no significant changes among our isolates in the hemagglutinin (H) gene, except for one substitution in the weasel isolate (W731F) (data not shown).

3.3. *Histopathology and immunohistopathology to detect CDV antigen*

The results of histopathological and immunohistopathological examinations of seven dead animals are summarized in Table 2. CDV antigens were detected in several of the organs and tissues examined; in No.734 and No.739, CDV antigens were mainly detected in the respiratory organs, but in No.744, most antigens were restricted to the digestive tissues. All of the organs in No.812 were positive for the CDV antigen (Fig. 1). The distribution of antigens was correlated with virus isolation (Tables 1 and 2).

3.4. *Comparison of H and F genes*

To assess the homogeneity among strains, 2022 bp fragments containing the H gene were amplified from W729B- and W812B-infected cells by RT-PCR using primers CDV-HF and CDV-HR (Demeter et al., 2007). The nucleotide sequences determined by direct sequencing are available under the accession numbers AB605890 (W729B) and AB605891 (W812B) which were deposited at the DNA Data Bank of Japan. Both H genes consisted of a 1824 bp region encoding 607 amino acids (Supplementary Fig. S2), and the identity between the nucleotide and amino acid sequences of W729B and W812B was 99.7% and 99.3%, respectively (data not shown). Interestingly, alignment of the deduced amino acid sequences of the H proteins showed that a substitution from tyrosine (Y) to histidine (H) was observed at position 549. This mutation is considered to have arisen in CDV as an adaptation to wild carnivores (Alex et al., 2007). The amino acid sequence of the signaling lymphocyte activation molecule (SLAM) receptor-binding region (amino acid residues 525–529) (Zipperle et al., 2010) was completely conserved (Supplementary Fig. S2). The amino acid sequences of our isolates showed 97–98% identity to other Asia-1 strains, 93–95% to other genotypes, and 90% to the Onderstepoort strain (data not shown).

Since the signal peptide region (amino acid residues 1–135) of the F protein is the most variable region of the CDV genome (Lee et al., 2010), the nucleotide sequences of this region were analyzed by direct sequencing. These sequence data are available under the accession numbers AB607904 (W729B) and AB607905 (W812B) in the DNA Data Bank of Japan. The results showed 99% identity among the signal peptide regions of our isolates, but only 73–82%

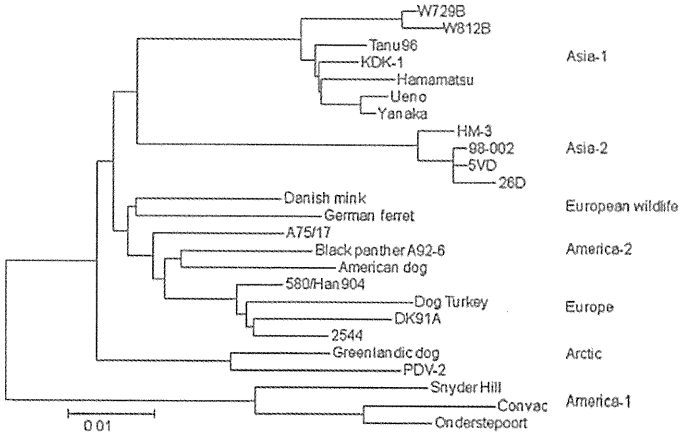

Fig. 2. Evolutionary relationship of CDV isolates inferred using the Neighbor-Joining method. Phylogenetic analysis was performed using a total of 607 amino acid positions with the MEGA4 program. Genotypes are indicated on the right. Accession numbers of the sequences used are BAA33740 (Tanu96), BAA84209 (KDK-1), BAA19585 (Hamamatsu), BAA19584 (Ueno), BAA19586 (Yanaka), BAB39167 (HM-3), BAA84208 (98-002), AAQ63642 (5VD), BAB39166 (26D), CAA87688 (Danish mink), CAA59358 (German ferret), AAD49703 (A75/17), CAA90879 (Black panther A92-6), CAA87691 (American dog), CAA59359 (5804/Han90), AAM11476 (Dog Turkey), AAQ05829 (DK91A), CAB01252 (2544), CAA87689 (Greenlandic dog), CAA59357 (PDV-2), AAG15490 (Snyder Hill), CAA84626 (Convac), AAK54669 (Onderstepoort). Scale bar indicates the number of nucleotide substitutions per site.

identity with amino acid sequences of other reported strains. In particular, amino acid sequence homology with the Onderstepoort vaccine strain was as low as 65–66% (data not shown).

3.5. Phylogenetic analysis of CDV isolates

Phylogenetic analysis of the predicted H proteins was performed to elucidate the evolutionary relationships between the CDV isolates of this study and other strains. Both of the isolates, W729B and W812B, from this CDV epizootic formed a common cluster and were classified as belonging to the Asia-1 genotype (Fig. 2).

3.6. Detection of antibodies against CDV in wild animals

To clarify CDV infection among wild animals in the vicinity of Tanabe, serum samples of feral animals were collected from 2007 to 2008 after the epizootic and a plaque reduction neutralization test ($PRNT_{75}$) was performed (Table 3, Supplementary Tables S1–S3). The results showed that 54 of 104 raccoons (52%) and four of 19 raccoon dogs (21%) possessed VN antibody to CDV strain KDK-1 (genotype Asia-1). In addition, two of five Sika deer (40%), 11 of 41 wild boars (27%), both of which belong to the *Artiodactyla*, and one badger, one Japanese marten, one Siberian weasel were also VN antibody-positive. The one fox and one weasel sampled had no VN antibody to CDV. However, CDV positivity in wild boars and Sika deer captured from 2009 to 2010 reduced to 4% and 0%, respectively (Table 3).

3.7. High seroprevalence of CDV in raccoons

Half of the raccoons (52%) were seropositive for CDV. The data for the raccoons were categorized according to capture locality, sex, and body weight (Table 4). Significant differences were observed between CDV seroprevalence and capture locality or body weight; raccoons in Tanabe (60%) showed significantly higher levels of seropositivity for CDV than those in cities surrounding Tanabe (41%) ($p < 0.05$) and adult raccoons (>4 kg; 76%) showed significantly higher levels of seropositivity for CDV than young raccoons (<4 kg; 43%) ($p < 0.05$). In addition,

Table 3
Seroprevalence of CDV in wild animals.

Animals	2007–2008		2009–2010	
	No. of examined animals	% of CDV-positive animals	No. of examined animals	% of CDV-positive animals
Raccoon (*Procyon lotor*)	104	52	–	–
Raccoon dog (*Nyctereutes procyonoides*)	19	21	–	–
Badger (*Meles meles*)	2	50	–	–
Weasel (*Mustela itatsi*)	1	0	–	–
Martes (*Martes melampus*)	1	100	–	–
Siberian weasel (*Mustela itatsi sibirica*)	1	100	–	–
Fox (*Vulpes vulpes*)	1	0	–	–
Wild boar (*Sus scrofa*)	41	27	28	4
Sika deer (*Cervus nippon*)	5	40	20	0

Table 4
Seroprevalence of CDV in raccoons.

	Cities		Sex		Body weight (kg)		Total
	Tanabe	Other	Male	Female	–3.9	4.0–	
No. of examined raccoons	58	46	61	43	75	29	104
No. of CDV-positive raccoons	35	19	35	19	32	22	54
% of CDV-positive raccoons	60	41	57	44	43	76	52

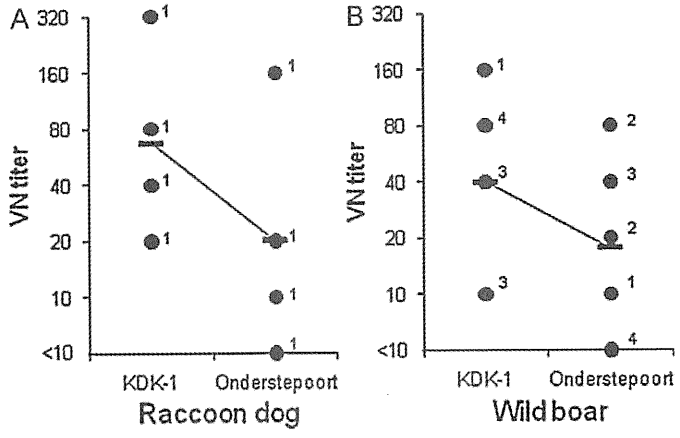

Fig. 3. VN titers to KDK-1 and Onderstepoort in wild boars and raccoon dogs. Sera from CDV (KDK-1)-seropositive wild boars and raccoon dogs were examined for VN titers to KDK-1 and Onderstepoort by $PRNT_{75}$. Horizontal bars show geometric mean of VN titer. Numbers show the number of animals with same VN titer.

comparisons of VN titers to KDK-1 and Onderstepoort in CDV-positive raccoons possessing high VN titers to KDK-1 (over 1:640) revealed that 70% of raccoons possessed VN titers to KDK-1 that were more than 4-fold greater than VN titers to Onderstepoort (Supplementary Table S1).

3.8. Seroprevalence of CDV in raccoon dogs

In raccoon dogs, only four animals (21%) possessed VN antibodies to CDV. No significant differences were observed in the seroprevalence of CDV between capture locality, sex, and body weight because the number of captured animals was too small (data not shown). Comparisons of the geometric mean titer of VN to KDK-1 and Onderstepoort among CDV-seropositive raccoon dogs revealed that the VN titer to KDK-1 was significantly higher than the VN titer to Onderstepoort ($p < 0.05$) (Fig. 3, Supplementary Table S3).

3.9. CDV-positivity in wild boars and Sika deer

A quarter of the wild boars (27%) sampled possessed VN antibodies to CDV. Examining the data by sex and body weight revealed that there was a significant difference in seroprevalence among animals with different body weights (Supplementary Table S2) ($p < 0.05$). More adult wild boars (>50 kg; 55%) were seropositive than young wild boars (<50 kg; 17%), and no significant difference was observed between sexes. In addition, comparison of the geometric mean titer of VN to KDK-1 and Onderstepoort among CDV antibody-positive wild boars revealed that the VN titer to KDK-1 was significantly higher than the VN titer to Onderstepoort ($p < 0.05$) (Fig. 3, Supplementary Table S3). In Sika deer, two animals possessed VN antibodies to KDK-1 and the VN titers of the CDV-positive sera were very low, 1:20 and 1:80 (Supplementary Table S3). In order to detect CDV-specific immunoglobulin in wild boars and Sika deer, ELISA was developed using lysate of KDK-1-infected Vero cells as an antigen and horseradish peroxidase-conjugated anti-swine immunoglobulin (MP Biomedicals, OH, USA) or anti-deer immunoglobulin (KPL, MD, USA) as secondary antibodies. The result showed that ELISA could also detect CDV-specific antibody in VN antibody-positive wild boars and Sika deer (data not shown).

4. Discussion

This study showed that the CDV epidemic occurred among many animal species in Tanabe. To our knowledge, this is the first report of a CDV epidemic in this region, implying that CDV may have been carried to Tanabe by a CDV-infected mammal, or that CDV may have jumped to wild mammals from a domestic dog in Tanabe.

Raccoon dogs seem to be highly susceptible to CDV infection, exhibiting high morbidity and mortality after infection. Indeed, a CDV epidemic in raccoon dogs presenting with pneumonia and gastroenteritis has been reported previously in Japan (Machida et al., 1993). In this study, eight of the raccoon dogs sampled died due to CDV infection. The lower seropositivity of CDV-positive raccoon dogs (21%) compared to raccoons (52%) may indicate that most of the raccoon dogs infected with CDV died before they were captured. Although finding dead wild animals is

difficult, the increased sensitivity and relatively high numbers of raccoon dogs would mean that, among wild animals, raccoon dogs may be well suited for use as indicators of an CDV epidemic in Japan.

On the other hand, raccoons exhibited the highest seropositivity to CDV, indicating that most of the raccoons sampled survived CDV infection during this epidemic. In North America, raccoons are considered to be important carriers of CDV and are responsible for transmission of the virus to other wild animals and domestic animals (Appel et al., 1994; Lednicky et al., 2004). Raccoons are exotic species in Japan and populations of this introduced species have increased rapidly in recent years. In Tanabe, the number of raccoons being captured is increasing (Sato and Suzuki, 2006), and it is possible that this increase in the raccoon population may be responsible for the transmission of CDV to other wild animals or that a single raccoon may have carried CDV to this area.

The wild boar and Sika deer sampled in this study both possessed VN antibodies to CDV. Only one report of CDV transmission to a peccary (suborder *Suina*) has been published to date (Appel et al., 1991), and no reports of CDV transmission to deer are known in the literature. Since wild boars are omnivores, they may become infected by either eating or coming into direct contact with diseased animals. Conversely, since deer are herbivores, they are unlikely to become infected by CDV through their feeding activity; however, they may come into contact with CDV-infected carnivores, such as raccoons and raccoon dogs. Further study is therefore required in order to clarify the route of CDV infection to these animals, particularly since the potential host range of CDV may be larger than we expect (Harder and Osterhaus, 1997).

Since antibody to CDV is cross-reactive to other morbilliviruses such as measles virus (MeV), rinderpest virus (RPV), peste-des-petitis ruminants virus (PPRV) and so on, it is difficult to deny the possibility that these CDV-positive animals were infected with other morbilliviruses. However, these morbilliviruses were serologically cross-reactive each other in VN test using hyperimmunized animal sera or some monoclonal antibodies, but in RPV-infected cattle and MeV-infected monkey, VN activity to CDV was less than detectable level (Sato et al., 1981). In addition, CDV-positive wild boars and Sika deer in 2009–2010 were 4% and 0% (Table 3), respectively, indicating that wild boars and Sika deer had not been infected with CDV or CDV-like virus after the CDV epidemic and that CDV might be only a morbillivirus to infect these animals around Tanabe city. These results strongly suggest that wild boars and Sika deer around Tanabe city must be infected with CDV, but not other morbilliviruses, during this epidemic.

All of the isolates obtained from wild animals belonged to genotype Asia-1. Phylogenetic analysis revealed that W812B isolated in 2008 had undergone more mutations than W729B in 2007, suggesting that a CDV epizootic among wild animals lasting 1 year could induce CDV evolution. When compared to the Onderstepoort vaccine strain, the amino acid sequence of the H proteins sequenced in this study exhibited lower homology (about 90%). In VN tests, cross-reactivity of the KDK-1 field isolate was lower than that observed with the Onderstepoort vaccine strain (Fig. 3), suggesting that the vaccine may become less effective for preventing field isolates of CDV due to the accumulation of mutations in the CDV infecting wild animals. It is therefore important to consider the evolution of CDV in order to develop of new vaccine strains.

We also observed a single amino acid mutation, from Y to H, at site 549 (Y549H) in our isolates. It has recently been reported that this mutation (Y549H) in the binding domain of SLAM (CD150) is associated with the spread of CDV to non-canine hosts (McCarthy et al., 2007). The findings of this study indicate that the change in residue 549 may affect the affinity between the CDV H protein and SLAM, increasing the potential of these mutants to infect wild animals.

In conclusion, CDV infection was found in several species of wild animals in Japan. In addition, a decrease was observed in both the homology of the H protein and cross-reactivity with the vaccine strain. Recent reports of CDV-induced mortality among rhesus monkeys in China and Japan (Morikawa et al., 2008; Sun et al., 2010) emphasize the need to monitor CDV in wild animals, clarify the host range of CDV, and improve the effectiveness of the CDV vaccine.

Acknowledgements

We thank Dr. Masami Mochizuki (Kyoritsu Seiyaku Corporation) for kindly providing us with KDK-1 strain. This study was supported by Grants-in-Aid from the Ministry of Education, Culture, Sports, Science and Technology of Japan and from the Innovation Center of Yamaguchi University.

Appendix A. Supplementary data

Supplementary data associated with this article can be found, in the online version, at doi:10.1016/j.vetmic.2011.07.006.

References

Appel, M.J., 1969. Pathogenesis of canine distemper. Am. J. Vet. Res. 30, 1167–1182.

Appel, M.J., Reggiardo, C., Summers, B.A., Pearce-Kelling, S., Maré, C.J., Noon, T.H., Reed, R.E., Shively, J.N., Örvell, C., 1991. Canine distemper virus infection and encephalitis in javelinas (collared peccaries). Arch. Virol. 119, 147–152.

Appel, M.J., Summers, B.A., 1995. Pathogenicity of morbilliviruses for terrestrial carnivores. Vet. Microbiol. 44, 187–191.

Appel, M.J., Yates, R.A., Foley, G.L., Bernstein, J.J., Santinelli, S., Spelman, L.H., Miller, L.D., Arp, L.H., Anderson, M., Barr, M., 1994. Canine distemper epizootic in lions, tigers, and leopards in North America. J. Vet. Diagn. Invest. 6, 277–288.

Demeter, Z., Lakatos, B., Palade, E.A., Kozma, T., Forgách, P., Rusvai, M., 2007. Genetic diversity of Hungarian canine distemper virus strains. Vet. Microbiol. 122, 258–269.

Harder, T.C., Osterhaus, A.D.M.E., 1997. Canine distemper virus—a morbillivirus in search of new hosts? Trends Microbiol. 5, 120–124.

Hirama, K., Goto, Y., Uema, M., Endo, Y., Miura, R., Kai, C., 2004. Phylogenetic analysis of the hemagglutinin (H) gene of canine distemper viruses isolated from wild masked palm civets (*Paguma larvata*). J. Vet. Med. Sci. 66, 1575–1578.

Lednicky, J.A., Dubach, J., Kinsel, M.J., Meehan, T.P., Bocchetta, M., Hungerford, L.L., Sarich, N.A., Witecki, K.E., Braid, M.D., Pedrak, C., Houde,

C.M., 2004. Genetically distant American canine distemper virus lineages have recently caused epizootics with somewhat different characteristics in raccoons living around a large suburban zoo in the USA. Virol. J. 1, 2.

Lee, M.S., Tsai, K.J., Chen, L.H., Chen, C.H., Liu, Y.P., Chang, C.C., Lee, S.H., Hsu, W.L., 2010. The identification of frequent variations in the fusion protein of canine distemper virus. Vet. J. 183, 184–190.

Machida, N., Izumisawa, N., Nakamura, T., Kiryu, K., 1992. Canine distemper virus infection in a masked palm civet (*Paguma larvata*). J. Comp. Pathol. 107, 439–443.

Machida, N., Kiryu, K., Oh-ishi, K., Kanda, E., Izumisawa, N., Nakamura, T., 1993. Pathology and epidemiology of canine distemper in raccoon dogs (*Nyctereutes procyonoides*). J. Comp. Pathol. 108, 383–392.

Martella, V., Elia, G., Lucente, M.S., Decaro, N., Lorusso, E., Banyai, K., Blixenkrone-Moller, M., Lan, N.T., Yamaguchi, R., Cirone, F., Carmichael, L.E., Buonavoglia, C., 2007. Genotyping canine distemper virus (CDV) by a hemi-nested multiplex PCR provides a rapid approach for investigation of CDV outbreaks. Vet. Microbiol. 122, 32–42.

McCarthy, A.J., Shaw, M.A., Goodman, S.J., 2007. Pathogen evolution and disease emergence in carnivores. Proc. Biol. Sci. 274, 3165–3174.

Mochizuki, M., Hashimoto, M., Hagiwara, S., Yoshida, Y., Ishiguro, S., 1999. Genotypes of canine distemper virus determined by analysis of the hemagglutinin genes of recent isolates from dogs in Japan. J. Clin. Microbiol. 37, 2936–2942.

Morikawa, S., Fukushi, S., Kurane, I., Sakai, K., Ami, K., Yamada, S., Hasegawa, H., Nagata, N., Sata, T., Matsui, S., Okabe, N., Nakajima, K., 2008. Outbreak of deadly canine distemper virus infection among imported cynomolgus (crab-eating) monkeys. IASR 29, 315 (in Japanese).

Nakano, H., Kameo, Y., Andoh, K., Ohno, Y., Mochizuki, M., Maeda, K., 2009a. Establishment of canine and feline cells expressing canine signaling lymphocyte activation molecule for canine distemper virus study. Vet. Microbiol. 133, 179–183.

Nakano, H., Kameo, Y., Sato, H., Mochizuki, M., Yokoyama, M., Uni, S., Shibasaki, T., Maeda, K., 2009b. Detection of antibody to canine distemper virus in wild raccoons (*Procyon lotor*) in Japan. J. Vet. Med. Sci. 71, 1661–1663.

Ohashi, K., Iwatsuki, K., Murata, K., Miyashita, M., Hukumoto, Y., Nakamura, K., Wakasa, C., Takahashi, E., Kai, C., 2001. Properties of a new CDV isolate from a raccoon dog (Nyctereutes procyonoides viverrinus) in Japan. Vet. Rec. 148, 148–150.

Roelke-Parker, M.E., Munson, L., Packer, C., Kock, R., Cleaveland, S., Carpenter, M., O'Brien, S.J., Pospischil, A., Hofmann-Lehmann, R., Lutz, H., 1996. A canine distemper virus epidemic in Serengeti lions (*Panthera leo*). Nature 379, 441–445.

Sato, H., Suzuki, K., 2006. Gastrointestinal helminths of feral raccoons (*Procyon lotor*) in Wakayama Prefecture, Japan. J. Vet. Med. Sci. 68, 311–318.

Sato, T.A., Hayami, M., Yamanouchi, K., 1981. Analysis of structural proteins of measles, canine distemper, and rinderpest viruses. Jpn. J. Med. Sci. Biol. 34, 355–364.

Sun, Z., Li, A., Ye, H., Shi, Y., Hu, Z., Zeng, L., 2010. Natural infection with canine distemper virus in hand-feeding Rhesus monkeys in China. Vet. Microbiol. 141, 374–378.

Takayama, I., Kudo, M., Takenaka, A., Fujita, K., Sugiyama, T., Arai, T., Yoneda, M., Sato, H., Yanai, T., Kai, C., 2009. Pathological and phylogenetic features of prevalent canine distemper viruses in wild masked palm civets in Japan. Comp. Immunol. Microbiol. Infect. Dis. 32, 539–549.

Timm, S.F., Munson, L., Summers, B.A., Terio, K.A., Dubovi, E.J., Rupprecht, C.E., Kapil, S., Garcelon, D.K., 2009. A suspected canine distemper epidemic as the cause of a catastrophic decline in Santa Catalina Island foxes (*Urocyon littoralis catalinae*). J. Wildl. Dis. 45, 333–343.

United States Fish and Wildlife Service, 2004. Endangered and threatened wildlife and plants; listing the San Miguel Island fox, Santa Rosa Island fox, Santa Cruz Island fox, and Santa Catalina Island fox as endangered. Fed. Reg. 69, 10335–10353.

Yoshizawa, M., Watabe, T., 2007. The canine distemper outbreak situation of mammals in Kochi City and the outskirts. Kagawa Seibutsu 34, 63–67 (in Japanese).

Watabe, T., Yoshizawa, M., 2006. The outbreak of death frequent occurrence of the wild raccoon dog by canine distemper. J. Environ. Dis. 15, 11–14.

Zipperle, L., Langedijk, J.P., Orvell, C., Vandevelde, M., Zurbriggen, A., Plattet, P., 2010. Identification of key residues in virulent canine distemper virus hemagglutinin that control CD150/SLAM-binding activity. J. Virol. 84, 9618–9624.

[技術コーナー]

Capnocytophaga canimorsus および *Capnocytophaga cynodegmi* 国内分離株の簡易同定キットを用いた同定法の検討

鈴木道雄・木村昌伸・今岡浩一・山田章雄
国立感染症研究所獣医科学部

(平成23年2月21日受付，平成23年8月5日受理)

国内の患者から分離された12株を含む計24株の *Capnocytophaga canimorsus* および国内の動物由来の6株を含む計7株の *Capnocytophaga cynodegmi* について，生化学的性状による簡易同定キットであるIDテスト・HNニッスイ-20ラピッド「ニッスイ」を用いた同定結果を検討した。*C. canimorsus* については，5%ウサギ血液加ハートインフュージョン寒天培地による増菌後の検査では24株中18株が *C. canimorsus* と同定され，また5株で *C. canimorsus* が鑑別候補菌種と判定された。糖の分解能に変異のあった1株は *C. cynodegmi* と同定された。24株中4株がβ-ラクタマーゼ陽性であった。また，*C. cynodegmi* については，7株中5株が *C. cynodegmi* と同定され，2株で *C. cynodegmi* が鑑別候補菌種と判定された。*C. canimorsus* および *C. cynodegmi* の菌種レベルでの確実な同定には遺伝子検査が必要であるが，簡易同定キットを用いた生化学的性状検査は検査室で簡便に実施することが可能であり，検査前に適切な増菌培養を行えば，*Capnocytophaga* 属菌をかなり高率に同定できることが示された。

Key words: *Capnocytophaga canimorsus*, *Capnocytophaga cynodegmi*, 簡易同定キット，5%ウサギ血液加ハートインフュージョン寒天培地，チョコレート寒天培地

Capnocytophaga 属菌は糸状のグラム陰性桿菌であり，二酸化炭素要求性および寒天培地上での滑走能を有すること，栄養要求性が厳しく成育が遅いことが特徴である。現在8種が知られており，うち6種はヒトの口腔内常在菌で，それら以外の2種，*C. canimorsus*, *C. cynodegmi* がイヌ・ネコの口腔内常在菌である。どちらもヒトに対して病原性を有するが，ヒトの重症例のほとんどは *C. canimorsus* 感染が原因である[1,2]。われわれが行った調査では，国内のイヌの74%，ネコの57%が *C. canimorsus* を保有していた[3]。

C. canimorsus 感染症は1976年にアメリカのBoboら[4]が世界で初めて報告して以来，世界で約250例の症例が報告されており，その致死率は約30%である[1,2]。わが国では1993年以来，23例（うち死亡例7例）の文献報告がある[1]。デンマーク，オランダでの疫学報告では人口100万人あたりそれぞれ0.5, 0.67人の患者がいると推定されている[4,5]。菌の生育が遅く，菌の分離が難しいことなどから，把握できていない症例も一定数あると考えられる。

C. canimorsus の同定に際しては，まず観察・鏡検時の特徴として，菌体の形態，コロニー形状が挙げられる。菌体の形態は糸状ないし紡錘形であり，*Fusobacterium nucleatum* に類似する。*Capnocytophaga* 属菌は滑走能を有することから，生育するにつれて，コロニーの辺縁が周囲へ拡がる特徴があるが，これは菌株や培養条件によって差異が大きく，*C. canimorsus* の臨床分離株においてはあまり明瞭に観察されないことが多い。菌体やコロニーの形状で同定することは難しく，菌種レベルでの同定にはPCR法が有用である[2,3]。臨床検査室で簡便に実施可能な同定検査としては，生化学的性状検査がある。簡易同定用キットは，各生化学的性状の陽性・陰性パターンにより細菌の属や種を判別するものであり，国内でも多くの種類が市販されている。その中でもIDテスト・HNニッスイ-20ラピッド「ニッスイ」(HNニッスイ-20ラピッド)

著者連絡先：(〒162-8640) 東京都新宿区戸山1-23-1
国立感染症研究所獣医科学部
鈴木道雄
TEL: 03-4582-2751
FAX: 03-5285-1179
E-mail: michios@nih.go.jp

は，結果判定用コードブックに *Capnocytophaga* 属菌が菌種レベルで収載されており，同属菌の菌種同定に有用であると思われたため，今回われわれは，国内の *C. canimorsus* 感染症患者からの臨床分離株および *C. canimorsus*, *C. cynodegmi* イヌ・ネコ分離株について，HN-20 ラピッドを用いて生化学的性状による同定結果を検討した。またその際，*Capnocytophaga* 属菌は栄養要求性が高いことから，*Capnocytophaga* 属菌が良好に発育する 5% ウサギ血液加ハートインフュージョン寒天培地（rb 加 HI 培地）と HN ニッスイ-20 ラピッドの主要な検査対象である *Haemophilus* 属菌および *Neisseria* 属菌などの増菌にも用いられ，臨床検査室でも汎用されているチョコレート寒天培地を用いて，検査結果に及ぼす増菌培地の影響も比較した。

供試菌株

国内の *C. canimorsus* 感染症患者からの臨床分離株 12 株 (H-1～12)，イヌ口腔内からの分離株 7 株 (D-1～7)，ネコ口腔内からの分離株 4 株 (C-1～4) および ATCC35979 株 (Type strain, A-1) の *C. canimorsus* 計 24 株，加えて *C. cynodegmi* のイヌ・ネコ口腔内分離株各 3 株 (D-8～10, C-5～7), ATCC49044 株 (Type strain, A-2) の計 7 株，総計 31 株を用いた（表 1)。供試菌株は，*C. canimorsus*, *C. cynodegmi* 特異的 PCR 検査の結果に基づいて菌種を決定した。また，供試菌株はいずれもオキシダーゼ陽性，カタラーゼ陽性であった。検査前の供試菌株の増菌には，われわれの研究室で分離・増菌培養に用いている，ハートインフュージョン粉末培地 (Difco) とウサギ脱繊血（日本バイオテスト社）を用いて自家で作製した rb 加 HI 培地および市販のチョコレート寒天培地 EX（チョコ培地）（日水製薬）を用いた（表 2)。それぞれの培地で 37℃, 5%CO_2 の培養条件下で 48 時間増菌培養したのち，HN ニッスイ-20 ラピッドに付属の HN ブイヨン

表 3. ID テスト・HN-20 ラピッド「ニッスイ」のテスト項目と点数によるコード化

ALA	アラニン　アミノペプチダーゼ	1	
PHO	ホスファターゼ	2	7
NIT	硝酸塩還元	4	
URE	尿素加水分解	1	
ODC	オルニチン　デカルボキシラーゼ	2	7
IND	インドール産生	4	
GLS	グルコシダーゼ	1	
PRO	プロリン　アミノペプチダーゼ	2	7
γGA	γ-グルタミル　アミノペプチダーゼ	4	
GLU	ブドウ糖分解	1	
MLT	麦芽糖分解	2	7
FRU	果糖分解	4	
MAS	マンノース分解	1	
MAN	マンニトール分解	2	7
TRE	トレハロース分解	4	
SUC	白糖分解	1	
LAC	乳糖分解	2	7
XYL	キシロース分解	4	
ONP	β-ガラクトシダーゼ	1	3
NIR	亜硝酸塩還元	2	
βLA	β-ラクタマーゼ	—	—

表 1. 供試菌株一覧

	菌株名		
C. canimorsus	ATCC35979	基準株 (Type strain)	アメリカ ATCC より購入
	H1～H12	ヒト患者分離株	国内分離株（2004～2010 年）
	D1～D7	イヌ口腔内分離株	国内分離株（2005～2007 年）
	C1～C4	ネコ口腔内分離株	国内分離株（2007 年）
	菌株名		
C. cynodegmi	ATCC49044	基準株 (Type strain)	アメリカ ATCC より購入
	D8～D10	イヌ口腔内分離株	国内分離株（2005～2007 年）
	C5～C7	ネコ口腔内分離株	国内分離株（2007 年）

表 2. 使用増菌培地

5% ウサギ血液加ハートインフュージョン寒天培地	rb 加 HI 培地	自家調製
チョコレート寒天培地 EX	チョコ培地	日水製薬

に，マクファランド3と同じ濃度になるように接種菌液を調製し，試験に供した。37℃好気条件下で4〜4.5時間反応後に各テスト項目（表3）の陽性・陰性を判定して，その結果をキットの用法に従って得点化し，7桁のコード番号を作成，コードブック ver. 1.02を参照して菌種の同定を行った。ヒト患者分離株についてはコードブックのAファイル（ヒト検体用）を，イヌ・ネコ口腔内分離株についてはBファイル（ヒト以外の検体用）をそれぞれ参照した。したがって，同じコード番号であってもヒト分離株とイヌ・ネコ分離株では鑑別対象となる菌種が異なる場合がある。また，セフィナーゼディスク（日本ベクトン・ディッキンソン）を用いて，各株のβ-ラクタマーゼ保有の有無を調べた。

C. canimorsus

rb加HI培地で増菌後の試験結果（表4）は，24株中18株が同定確率98%以上で *C. canimorsus* と同定され，2株(H-10, D-2)が *C. canimorsus* あるいは *C. cynodegmi* のいずれかであると同定された。一方残りの4株では，*C. canimorsus*, *C. cynodegmi* に加えてH-7株では *Gardnerella vaginalis* が，H-8株では *Capnocytophaga ochracea* が鑑別候補となった。C-3株では *C. canimorsus* に加えて *Avibacterium paragallinarum* が鑑別候補となった。D-1株はPCR検査では *C. canimorsus* と同定されているが，本試験では確率99%で *C. cynodegmi* と同定された。D-1株では通常 *C. canimorsus* では陽性にならないスクロース分解能が陽性であった。一方，チョコ培地で増菌した結果（表4）でも，3株(H-8, D-1, D-4)を除いて，14株が99%以上の確率で *C. canimorsus* と同定され，6株が *C. canimorsus* が2〜3種の鑑別候補菌種のうちの一つ（同定確率50〜60%台）と判定されたが，糖の分解能の項目ではrb加HI培地増菌では陽性だったものがチョコ培地増菌では陰性と判定される場合がしばしば認められた。また，H-7株がチョコ培地増菌ではコード番号表中に該当菌種なしとなり，D-4株は確率

表4. *C. canimorsus* 検査成績

菌株*	5%ウサギ血液加ハートインフュージョン寒天培地					チョコレート寒天培地EX				
	コード	同定菌名	確率	同定菌名	確率	コード	同定菌名	確率	同定菌名	確率
H-1	3010001	*C. canimorsus*	>99%	—		3010001	*C. canimorsus*	>99%	—	
H-2	3013121	*C. canimorsus*	98%	—		3010001	*C. canimorsus*	>99%	—	
H-3	3010001	*C. canimorsus*	>99%	—		3010001	*C. canimorsus*	>99%	—	
H-4	3001121	*C. canimorsus*	99%	—		3000001	*C. canimorsus*	>99%	—	
H-5	3001121	*C. canimorsus*	99%	—		3000001	*C. canimorsus*	>99%	—	
H-6	3013121	*C. canimorsus*	98%	—		3011101	*C. canimorsus*	99%	—	
H-7	3017161	*C. canimorsus*	62%	*C. cynodegmi*	31%	3010041	該当なし		—	
H-8	3037121	*C. ochracea*	53%	*C. canimorsus*	29%	3037121	*C. ochracea*	53%	*C. canimorsus*	29%
H-9	3013121	*C. canimorsus*	98%	—		3017121	*C. canimorsus*	64%	*C. cynodegmi*	32%
H-10	3017121	*C. canimorsus*	64%	*C. cynodegmi*	32%	3017121	*C. canimorsus*	64%	*C. cynodegmi*	32%
H-11	3013121	*C. canimorsus*	98%	—		3010001	*C. canimorsus*	>99%	—	
H-12	3010001	*C. canimorsus*	>99%	—		3010001	*C. canimorsus*	>99%	—	
D-1	3037171	*C. cynodegmi*	99%	—		3037171	*C. cynodegmi*	99%	—	
D-2	3017121	*C. canimorsus*	67%	*C. cynodegmi*	33%	3017161	*C. canimorsus*	67%	*C. cynodegmi*	33%
D-3	3013121	*C. canimorsus*	99%	—		3010001	*C. canimorsus*	54%	*A. paragallinarum*	46%
D-4	3013121	*C. canimorsus*	99%	—		1010001	*A. paragallinarum*	>99%	—	
D-5	3013121	*C. canimorsus*	99%	—		3013121	*C. canimorsus*	99%	—	
D-6	3013121	*C. canimorsus*	99%	—		3010001	*C. canimorsus*	54%	*A. paragallinarum*	46%
D-7	3050001	*C. canimorsus*	>99%	—		3050001	*C. canimorsus*	>99%	—	
C-1	3053121	*C. canimorsus*	99%	—		3053121	*C. canimorsus*	99%	—	
C-2	3013121	*C. canimorsus*	99%	—		3013121	*C. canimorsus*	99%	—	
C-3	3010001	*C. canimorsus*	54%	*A. paragallinarum*	46%	3010001	*C. canimorsus*	54%	*A. paragallinarum*	46%
C-4	3013121	*C. canimorsus*	99%	—		3013121	*C. canimorsus*	99%	—	
A-1	3013121	*C. canimorsus*	98%	—		3010001	*C. canimorsus*	>99%	—	

*: H-1–12: ヒト由来，D-1–7: イヌ由来，C-1–4: ネコ由来，A-1: ATCC35979株(Type strain)
3番目の候補菌種は表中省略（本文参照）